Redox Biology 28 (2020) 101375

Contents lists available at ScienceDirect

Redox Biology

journal homepage: www.elsevier.com/locate/redox

Research Paper

Loss of epitranscriptomic control of selenocysteine utilization engages senescence and mitochondrial reprogramming

May Y. Lee[a], Andrea Leonardi[b], Thomas J. Begley[a,b,c], J. Andrés Melendez[a,*]

[a] Nanobioscience Constellation, Colleges of Nanoscale Science & Engineering, SUNY Polytechnic Institute, 257 Fuller Rd., Albany, NY, 12203, USA
[b] Nanobioscience Constellation, Colleges of Nanoscale Science & Engineering, University at Albany, 257 Fuller Rd., Albany, NY, 12203, USA
[c] The RNA Institute, College of Arts & Sciences, University at Albany, 1400 Washington Ave., Albany, NY, 12222, USA

ARTICLE INFO

Keywords:
Epitranscriptome
Selenium
Senescence
Mitochondria
Uncoupling protein

ABSTRACT

Critically important to the maintenance of the glutathione (GSH) redox cycle are the activities of many selenocysteine-containing GSH metabolizing enzymes whose translation is controlled by the epitranscriptomic writer alkylation repair homolog 8 (ALKBH8). ALKBH8 is a tRNA methyltransferase that methylates the wobble uridine of specific tRNAs to regulate the synthesis of selenoproteins. Here we demonstrate that a deficiency in the writer ALKBH8 (*Alkbh8*^{def}), alters selenoprotein levels and engages senescence, regulates stress response genes and promotes mitochondrial reprogramming. *Alkbh8*^{def} mouse embryonic fibroblasts (MEFs) increase many hallmarks of senescence, including senescence associated β-galactosidase, heterocromatic foci, the cyclin dependent kinase inhibitor p16^{Ink4a}, markers of mitochondrial dynamics as well as the senescence associated secretory phenotype (SASP). *Alkbh8*^{def} cells also acquire a stress resistance phenotype that is accompanied by an increase in a number redox-modifying transcripts. In addition, *Alkbh8*^{def} MEFs undergo a metabolic shift that is highlighted by a striking increase in the level of uncoupling protein 2 (UCP2) which enhances oxygen consumption and promotes a reliance on glycolytic metabolism. Finally, we have shown that the Alkbh8 deficiency can be exploited and corresponding MEFs are killed by glycolytic inhibition. Our work demonstrates that defects in an epitransciptomic writer promote senescence and mitochondrial reprogramming and unveils a novel adaptive mechanism for coping with defects in selenocysteine utilization.

1. Introduction

The epitranscriptome can serve to regulate translation through post-transcriptional modification of RNAs and its dysregulation is associated with disease and toxicant susceptibility [1–6]. Alkylation repair homolog 8 (ALKBH8) is an epitranscriptomic writer with tRNA methyltransferase activity and it can methylate the wobble uridine on tRNA$^{Sec\ 7,8}$. ALKBH8 is required to complete the formation of 5-methoxycarbonylmethyluridine (mcm [5]U) and 5-methoxycarbonylmethyl-2′-O-methyluridine (mcm [5]Um), and these RNA modifications promote UGA-stop codon recoding which is needed for the incorporation of the rare 21st amino acid selenocysteine (Sec) [7–10]. We have shown that ALKBH8 protein levels, stop-codon recoding and ALKBH8-dependent uridine wobble base modifications are increased in response to reactive oxygen species (ROS) stress to improve the translation of selenocysteine containing glutathione peroxidase (GPX) and thioredoxin reductase (TRXR) enzymes [11], supporting the idea that the epitranscriptomic writer ALKBH8 is a ROS sensor and effector.

Senescence is a form of replicative arrest which is triggered by a variety of stressors including but not limited to DNA damage, telomere erosion, and oxidative stress [12]. While senescence is beneficial as an innate tumor-suppressive mechanism responsible for inducing permanent replicative arrest in cells at risk of malignant transformation, it has been established that the accumulation of senescent cells with increasing age is deleterious in tissue microenvironments *in vivo* [13]. Upon senescent transformation, cells adopt a modulated secretome termed the senescence-associated secretory phenotype (SASP), increasing secretion of inflammatory cytokines, matrix metalloproteinases (MMPs), chemokines, and growth factors into the surrounding tissue microenvironment [14]. Through its ability to evoke responses from cells in a paracrine fashion, SASP has been linked to numerous age-associated disease pathologies including tumor invasion, cardiovascular dysfunction, neuroinflammation, osteoarthritis and renal disease [15–18].

While there is wealth of information linking senescence to many degenerative disease processes [17–22] the role of selenium in the

* Corresponding author. Colleges of Nanoscale Science & Engineering, SUNY Polytechnic Institute, 257 Fuller Road, Albany, NY, 12203, USA.
E-mail address: jmelendez@sunypoly.edu (J.A. Melendez).

https://doi.org/10.1016/j.redox.2019.101375
Received 4 November 2019; Accepted 5 November 2019
Available online 11 November 2019

regulation of the senescence program has only recently been unveiled. Se supplementation can extend the replicative lifespan of cells in culture [23] and Se deprivation or supplementation can accelerate or delay the production of senescence associated markers, respectively [23–25]. While serum selenium levels are predictors of longevity and healthy aging [26–28] selenium deprivation has also been shown to promote longevity [29]. Selenium is functionally utilized by small repertoire of enzymes as Sec, which is incorporated translationally through the use of UGA stop codon recoding and under epitranscriptomic control. However, little is known with respect to the specific contribution of epitranscriptomic writers that control Sec utilization in regulating senescence. In this study, we show that deficiency in ALKBH8 engages senescence, mitochondrial reprogramming and confers a survival advantage to cells with a limited capacity to incorporate selenocysteine. Increases in selenoncysteine containing proteins are often associated with chemoresistance and these findings indicate that therapeutic strategies to impede selenoprotein activity may further accentuate drug resistance and confer and advantageous survival advantage.

2. Materials and methods

2.1. Cell culture

Both wild type (WT) Mouse Embryonic Fibroblasts (MEFs) and *Alkbh8* deficient (*Alkbh8*^{def} or *Def*) MEFs were cultured in Dulbecco's Modified Eagle's Medium (DMEM) (Corning Inc., Corning, NY) supplemented with 10% fetal bovine serum (Corning Inc., Corning, NY), 10% non-essential amino acids (Corning Inc., Corning, NY), 100 Units/mL penicillin and 100 μg/ml streptomycin, at 21% oxygen tension at 37 °C and 5% CO_2. These cells were lifted in 0.25% trypsin/EDTA (Corning Inc., Corning, NY) and serially passaged at a dilution of 1:6.

Primary human fetal lung fibroblasts (IMR90) were cultured in Minimum Essential Medium (MEM) (Corning Inc., Corning, NY) supplemented with 10% fetal bovine serum and incubated at 21% oxygen tension at 37 °C with 5% CO_2. These cells were lifted in 0.25% trypsin/EDTA and serially passaged at a dilution of 1:4.

To analyze cell viability in different oxygen concentration, cells were cultured in 21% and 3% O_2 for 5 days and counted every 24 h.

2.2. Cytotoxicity and colony formation

10,000 cells per well were seeded in 96 well plates (Celltreat, Pepperell, MA) and were treated for 24 h with 2 deoxy-glucose (2DG) (Cayman, Ann Arbor, MI) at indicated concentrations to measure cytotoxicity. Cells were then stained with crystal violet, followed by solubilizing with 10% acetic acid and absorbance was measured with Flex Station 3 plate reader (Molecular Devices, San Jose, CA) at a wavelength of 570 nm. 500 cells per well were seeded in 24 well plates with 0.31 mM 2DG. Cells were grown for 5 days and colonies formed were stained using crystal violet. Colonies of 15 or more cells were counted for quantification and surviving fraction was calculated as (number of colonies formed/500 cells plated).

2.3. Quantitative RT-PCR

In brief, total mRNA was extracted from respective cell lines using TRIzol reagents (Life Technologies, Carlsbad, CA) as described by manufacturer. cDNA was synthesized from 500 ng total mRNA using Maxima H Minus First strand kits (Thermo Fisher Scientific, Waltham, MA). Real-time quantitative RT-PCR was performed in triplicates on a 7500 PCR system (Applied Biosystems, Förster city, MA) and the sequences were described in Supplementary Table 1. Additional oxidative stress and antioxidant defense regulated genes were also analyzed using RT [2] profiler PCR array (Qiagen, Hilden, Germany).

2.4. Western blot

Cell were washed twice with cold phosphate-buffered saline (PBS) and lysed with radioimmunoprecipitation (RIPA) lysis buffer. The lysates were centrifuged for 15 min at full speed at 4 °C. For sample preparation, 15 μg of whole cell lysates were used and 6X SDS sample buffer with 10% of 0.5 M DTT added to each sample prior to boiling for 15 min. The samples were then separated on an 8% SDA-polyarylamide gel (Thermo Fisher Scientific, Waltham, MA) and transferred onto nitrocellulose membrane (Thermo Fisher Scientific, Waltham, MA). The membrane was blocked with 5% dry milk in 0.1% Tris-buffered saline-Tween 20 for 1 h and incubated overnight at 4 °C with primary antibodies, UCP2 (1:400) (Santa Cruz Biotechnology, Dallas, TX), Mitofusin 1 (1:500) (Cell Signaling Technology, Danvers, MA), Mitofusin 2 (1:500) (Cell Signaling Technology, Danvers, MA), Drp1 (1:500) (Cell Signaling Technology, Danvers, MA), GAPDH (1:10000) (Santa Cruz Biotechnology, Dallas, TX), Alkbh8 (1:1000) (ABclonal, Woburn, MA), GPX1 (1:1000) (R&D Systems, Minneapolis, MN), and TRXR2 (1:1000) (ABCAM, Cambridge, MA) followed by incubation with respective secondary antibodies, either anti-mouse (1:10000) (Cell Signaling Technology, Danvers, MA), anti-goat(1:10000) (ABCAM, Cambridge, MA) or anti-rabbit (1:10000) (Cell Signaling Technology, Danvers, MA) for 1 h. The membranes were developed by Supersignal West Femto Maximum sensitivity substrate kit (Thermo Fisher Scientific, Waltham, MA) and imaged with ChemiDoc™ imaging system (BIO-RAD, Hercules, CA).

2.5. SA-β-gal staining

Senescence Associated β-Galactatosidase (SA-β-Gal) staining was performed using senescence-galactosidase staining kit (Cell Signaling Technology, Danvers, MA) as per manufacturer's protocol. Briefly, cells were seeded in 6-well tissue culture plates overnight and washed once with PBS. 1 ml of 1x fixative solution was added and incubated for 15 min at room temperature. The plates were washed twice with PBS and stained with 1 ml of β -Gal staining solution for overnight at 37 °C in a dry non-CO_2 incubator. Images were taken in nine random fields using light microscopy and β-gal-positive cells are presented as intensity normalized to WT MEFs using ImageJ software.

2.6. Heterochromatin foci staining

Cells were seeded on coverslips in 6-well tissue culture plates overnight, followed by fixation of the cells with cold 4% formaldehyde solution for 15 min at room temperature. The plates were washed once with cold PBS and the coverslips were mounted on glass slides with Prolong™ Gold Antifade Mount containing DAPI (Thermo Fisher Scientific, Waltham, MA). The slides were left overnight to dry in the dark and sealed with clear nail polish. Images were taken in three random fields using florescent microscope and heterochromatin foci positive nuclei are presented as percentage of total number of counted nuclei.

2.7. Mitochondrial oxygen consumption rate

Oxygen Consumption rate (OCR), and extracellular acidification rate (ECAR) were measured at 37 °C as per manufacturer's protocol for the seahorse XF24 extracellular flux analyzer (Agilent Technologies, Santa Clara, CA). Briefly, cells were seeded in 24-well tissue culture plate overnight, allowing the cells to adhere. Due to differences in proliferative capacity between cell types, cells were seeded at differing densities so that cell numbers were equivalent at time of metabolic flux analysis. On the day of analysis, Cells were changed to conditional seahorse assay media at pH 7.4 supplemented with 25 mM glucose and 1 μM sodium pyruvate. Cells were incubated in non-CO_2 incubator at 37 °C for 1 h and respiration was measured before and after injection of

three compounds: oligomycin (1 μM), carbonyl cyanide 4-(trifluoromethoxy) phenylhydrazone (FCCP) (3 μM), and rotenone (1 μM). Immediately after the run, cells were lysed in RIPA buffer and the protein concentration was measured using BCA assay. The results were normalized with the protein OD value of corresponding wells and OCR, ECAR and cell energy phenotype were automatically calculated by Wave software (Agilent Technologies, Santa Clara, CA).

2.8. Mitotracker green staining

Cells were seeded on cover-slips for 24 h to reach desired confluency. The cells were then stained with 200 nM MitoTracker Green (Invitrogen, Carlsbad, CA) and incubated for 15 min at 37 °C. After incubation period, cells were washed once with PBS and fixed with 4% formaldehyde solution for 15 min at room temperature. The plates were then washed once with cold PBS and the coverslips mounted on glass slides with Prolong™ Gold Antifade Mount. The slides are immediately imaged using 60x oil immersion objective (Zeiss, Oberkochen, Germany). The morphology and the length of the mitochondria are measured using Fiji-ImageJ [30,31]. Briefly, MiNA macro tool was installed in Fiji from https://github.com/ScienceToolkit/MiNA as per instructions. After opening the images with Fiji software, granular noise is remover (process →Noise→Despeckle) and local contrast enhancement performed to improve the binary image quality, as well as better visualization of small, dendritic mitochondria (Process→Enhance Local Contrast (CLAHE). Plugins→Analyze→Tubeness was perform to see the mitochondrial network. And the morphology of the mitochondria were analyzed in following steps; Process→Binary→Make Binary, Process→Binary→skeletonize, Analyze→Skeleton→Analyze Skeleton(2D/3D), and Plugins→Stuart Lab→MiNA Scripts→MiNA Analyze Morphology.

2.9. 2′,7′-dichlorodihydrofluorescein diacetate (H_2DCFDA) staining

Cells were seeded in 96-well black/clear bottom plate with or without 20 μM genipin treatment overnight. On the day of assay, the cells were washed once with PBS, and treated with 300 μM H_2O_2 for 30 min at 37 °C. The cells were then washed once with PBS and stained with 30 μM cell-permeant oxidation-sensitive dye H_2DCFDA (Invitrogen, Carlsbad, CA) for 30 min at 37 °C, followed by fluorescence analysis (485 nm excitation, 535 nm emission) with Flex Station 3 plate reader. The oxidation-insensitive dye 5(6)-carboxyl-2′,7′-dichlorodihydrofluorescein diacetate (CDCF) (Invitrogen, Carlsbad, CA) was used as control so that any fluorescence changes between groups with H_2DCFDA is directly attributed to changes in the dye oxidation. Mean fluorescent values for H_2DCFDA-treatment cells were normalized to values of the control CDCF-treated cells.

2.10. Statistical methods

Data were analyzed using GraphPad Prism version 8 software. All statistical analyses were performed with the GraphPad Prism 8.0 statistical software package. Statistical significance was assessed using the two-tailed Student's *t*-test or one-way ANOVA with Tukey-Kramer post-test. P values of <0.05 were considered significant.

3. Results

3.1. Alkbh8 deficient cells engage cellular senescence

We have established *that Alkbh8* deficiency limits selenoprotein synthesis, elevating cellular ROS levels [11] (Supplementary Figure 1**)**, and that increases in steady state H_2O_2 production drive SASP [14]. We first performed a focused array using Qiagen's Oxidative Stress and Antioxidant Defense RT [2] Profiler PCR Array to evaluate potential adaptive oxidant metabolizing genes that aid in the survival of cells deficient in *Alkbh8* and the absence of many functional key

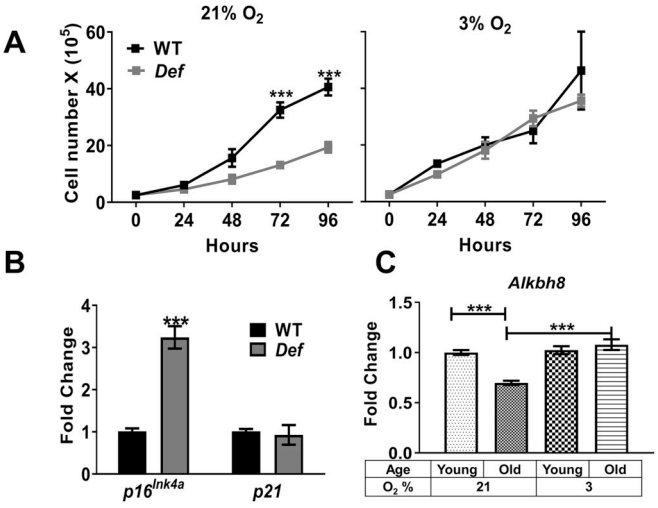

Fig. 1. *Alkbh8* deficiency impedes cell growth, induces *p16Ink4a* and is observed in senescent human diploid fibroblast IMR-90 cells. A) Growth of *Alkbh8*^{def} and WT MEFs in 21% and 3% O_2. **B)** RT-PCR transcript levels *p16*^{Ink4a} and *p21* from wild type (WT) and *Alkbh8 deficient (def)* cells. All data was normalized to *β-actin* controls. Data shown are the mean ± SEM, ***, $p \leq 0.001$ when compared to WT. **C)** RT-PCR transcript levels of *Alkbh8* from young and old (senescent) human diploid fibroblast IMR90 cells culture in low and high oxygen. Data shown are the mean ± SEM, ***, $p \leq 0.001$.

selenocysteine containing proteins. Supplementary Table 2 summarizes our findings indicating that there is a robust increase in the levels of number of key oxidant-metabolizing genes, including Superoxide dismutase 2 (*Sod2*), neutrophil cytosol factor1 (*Ncf1*), Uncoupling protein 2 and 3 (*Ucp2* and *Ucp3*) and glutathione peroxidase 3 and 6 (*Gpx3* and *Gpx6*). Indicating that selenoprotein deficiency is accompanied by adaptive increases in the transcripts of oxidant-metabolizing genes. We next evaluated whether the increased oxidizing capacity of *Alkbh8*^{def} cells activate the senescent program. We first characterized the proliferative capacity of *Alkbh8*^{def} cells as cellular senescence is accompanied by growth arrest. As shown in Fig. 1A, *Alkbh8*^{def} MEFs display a significant proliferative defect, compared to their WT controls, that is reversed by growth in low oxygen (3% O_2). The tumor suppressor *p16*^{INK4a} has been well established as a senescence marker and its expression was significantly upregulated in *Alkbh8*^{def} MEFs (Fig. 1B**)** while the cell cycle regulator *p21* was not. We next set out to determine if replicative senescence, which is observed in primary human diploid cells, is accompanied by alterations in the levels of *Alkbh8*. Transcript levels of *Alkbh8* were decreased in senescent IMR-90 human diploid fibroblasts, relative to pre-senescent cells, which was reversed by culturing cells in 3% O_2 (Fig. 1C). These, observations suggest that *Alkbh8* depletion is associated with proliferative defects linked to the senescence program.

Cellular senescence is also associated with the formation of heterochromatin foci (HCF), which are enriched in chromatin modifications. HCF can be monitored using high magnification fluorescence microscopy in combination with DAPI staining as in Fig. 2A, demonstrating significant enrichment of HCF in *Alkbh8*^{def} MEFs. Senescence associated beta-galactosidase (SA-β-gal) is also a key indicator of senescence engagement and can be detected at pH 6 in single cells using X-Gal staining [32]. *Alkbh8*^{def} cells display significant increases in SA-β-gal staining compared to WT (Fig. 2B**).** The senescence associated secretary phenotype is common to all forms of senescence and is causal to age-related decline in organ function [33]. We have established that the senescence associated secretory phenotype is under redox-control [14] and it is likely that oxidative stress that accompanies the impairment in selenoprotein exacerbates SASP. As shown in Fig. 3, the levels of many of the most prominent SASP markers are dramatically upregulated

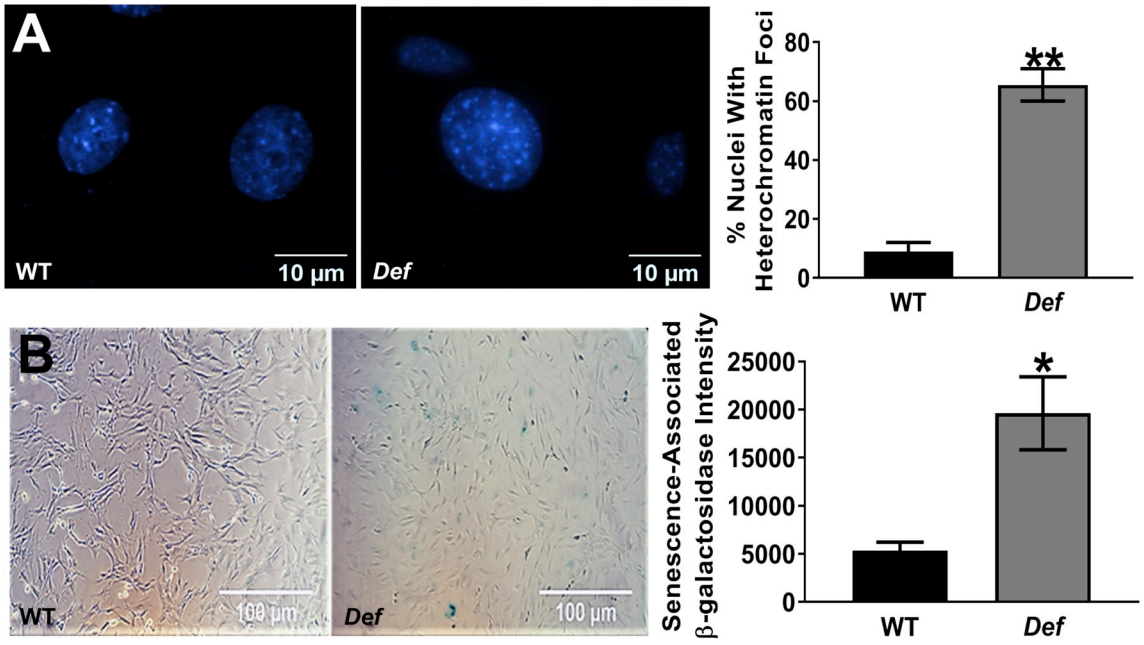

Fig. 2. *Alkbh8* deficiency increases senescence associated heterochromatic foci and senescence associated β-galactosidase levels. A) WT and *Alkbh8*^{def} MEFs stained with DAPI (*left panels*) and imaged at differing fluorescence intensities (upper and lower panels) to accentuate stained nuclei. Quantification of HCF ($n = 5$), (*right panel*). **B)** Senescence-Associated β-galactosidase staining of WT and Alkbh8^{def} MEFs (*left panels*) and quantification ($n = 3$), (*right panel*). Data shown are the mean ± SEM, **, $p \leq 0.01$ and *, $p \leq 0.05$ for A and B, respectively.

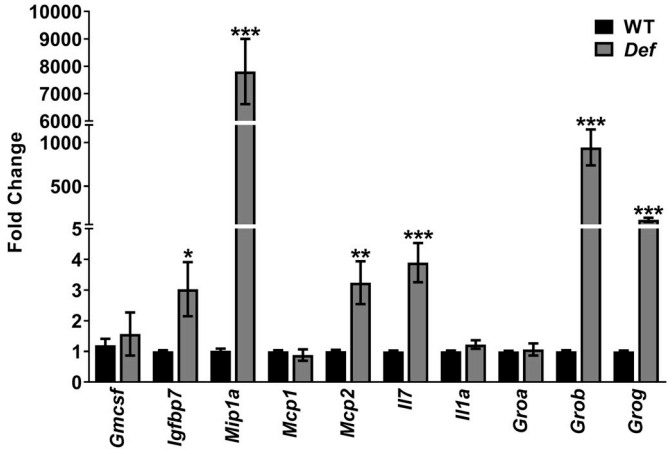

Fig. 3. *Alkbh8* deficiency engages the Senescence Associate Secretory Phenotype. RT-PCR of indicated SASP transcripts in control and *Alkbh8*^{def} MEFs (n = 3). Data shown are the mean ± SEM, *, $p \leq 0.05$, **, $p \leq 0.01$, ***, $p \leq 0.001$ when compared to WT.

when selenocysteine utilization is impaired by *Alkbh8* deficiency. Further, Alkbh8 rescue negated any increases in SASP and HCF observed in the *Alkbh8*^{def} cells (Supplementary Figure 2). Thus, *Alkbh8* deficiency is clearly responsible for the increase in senescent marks.

3.2. Alkbh8 deficiency engages mitochondrial reprogramming

Mitochondrial fusion has also been shown to play an important role in adapting to stress and increased fusion events are correlated with senescence [34,35]. To determine if a deficiency in the epitranscriptomic writer ALKBH8 alters mitochondrial morphology, we performed mitochondrial staining using mitotracker green in combination with Fiji-ImageJ. *Alkbh8*^{def} cells display a significant increase in mean mitochondrial length and mean summed branch length when compared to WT, while other mitochondrial network parameters remain the same. (Fig. 4A, Supplementary Fig. 3). Fusion serves a protective function in response to cell stress [36] and is controlled by key fusion (MFN1, MFN2 and OPA1) and fission associated proteins (FIS1 and DRP1). Analysis of a subset these fusion and fission proteins revealed no change in the levels of the fusion proteins MFN1 and MFN2 but a striking decrease in the levels of the fission protein DRP1 (Fig. 4B) in *Alkbh8*^{def} cells. Decreases in the levels of fission to fusion related proteins may in part explain the elongated mitochondrial structure in the *Alkbh8* deficient MEFs. Overall, the above findings support the idea that mitochondria play an important role in adapting to epitranscriptomic defects.

3.3. Alkbh8 deficiency engages mitochondrial reprogramming

The resulting increase in mitochondrial length that accompanies *Alkbh8* deficiency led us to investigate mitochondrial function. We monitored mitochondrial oxygen consumption and glycolytic flux in *Alkbh8*^{def} MEFs using the XF24 Analyzer (Seahorse Biosciences). Due to differences in proliferative capacity between cell types (Fig. 1A) and the need for standard 24-h plate equilibration, cells were seeded at differing densities so that cell numbers were equivalent at time of metabolic flux analysis. *Alkbh8*^{def} MEFs display significant increases in basal, maximal and non-mitochondrial respiration and extracellular acidification compared to WT MEFs (Fig. 5A and B). The cell energy phenotype indicates that *Alkbh8*^{def} MEFs display energetic adaptation utilizing both aerobic and glycolytic metabolism in response to mitochondrial stress (Fig. 5C) which is also reversed by *Alkbh8* rescue (Supplementary Fig. 4).

3.4. UCP2 plays a role in mitochondrial adaptation observed in Alkbh8^{Def}

Uncoupling protein 2 (*Ucp2*) was one of the most highly expressed genes in our focused array analyses and its expression has been reported to increase upon irradiation induced senescence [37], thus we tested whether its upregulation might explain the altered functional activity of mitochondria in the *Alkbh8*^{def} cells. UCP2, is found in the inner mitochondrial membrane and plays a key role in uncoupling ATP synthase from electron transport chain as well as in limiting mitochondrial ROS

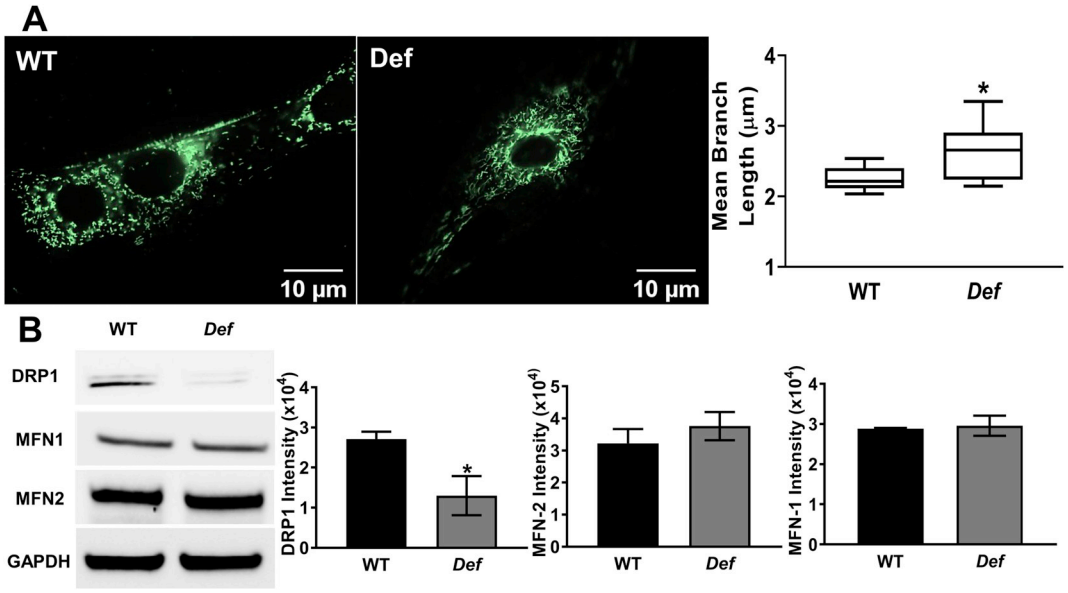

Fig. 4. *Alkbh8* deficiency is accompanied by increases in mitochondrial length which is associated with a decrease in fission related protein DRP1. A) WT and *Alkbh8*^{def} MEFs were stained with 200 nM Mitotracker green for 15 min and live-imaged using Zeiss Z1 inverted fluorescence microscope. The lengths of 100 randomly selected mitochondrial were measured using ImageJ (n = 10). The box plots show median (middle Horizontal lines), first to third quartile (box), and min and max (outer horizontal lines) with *, $p \leq 0.05$. **B)** Immunoblot analysis of fission and fusion proteins from WT and *Alkbh8*^{def} cells and accompanying quantitative analysis (n = 3). Data shown are the mean ± SEM, ***, $p \leq 0.001$ for mitochondrial length and *, $p \leq 0.05$ for DRP1. (For interpretation of the references to colour in this figure legend, the reader is referred to the Web version of this article.)

production by decreasing electron leak [38]. We first confirmed its expression at both the transcript and protein levels (Fig. 6A). Interestingly, limiting metabolic oxygen exposure with low oxygen (3% O_2) tempered the elevations in Ucp2 expression that accompany Alkbh8 deficiency. The effects of elevated UCP2 on mitochondrial function vary and both inhibitory as well stimulatory activity have been observed [39].

We next measured mitochondrial oxygen consumption and extracellular acidification in *Alkbh8*^{def} MEFs but in the presence and absence of the UCP2 inhibitor genipin. As in Fig. 5, *Alkbh8*^{def} MEFs display significant increases in basal, maximal and non-mitochondrial respiration and extracellular acidification compared to WT MEFs, both of which are negated by treatment with UCP2 inhibitor, genipin (Fig. 6B). In addition, the cell energy phenotype indicates that *Alkbh8*^{def} MEFs display energetic adaptation utilizing both aerobic and glycolytic metabolism in response to mitochondrial stress and this adaptation is

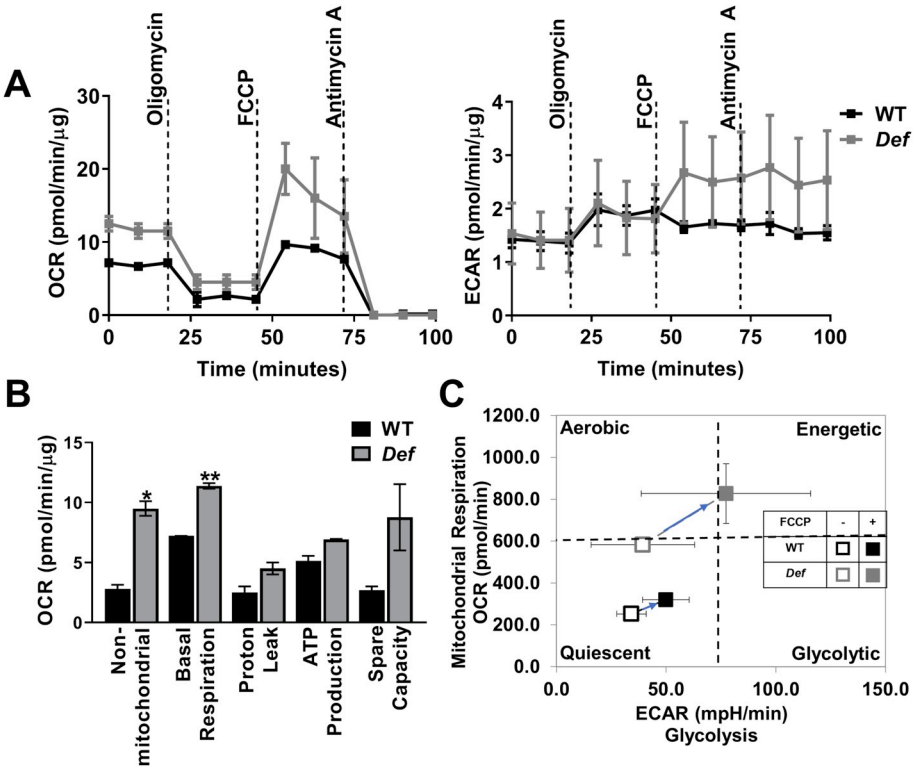

Fig. 5. *Alkbh8* deficiency is accompanied by an increase oxygen consumption and extracellular acidification. A) Extracellular Flux analysis of WT and *Alkbh8*^{def} MEFs using XF24 analyzer. The graphs represent the kinetic profiles of oxygen consumption rate (OCR), and extracellular acidification rate (ECAR) in WT and *Alkbh8*^{def} MEFs. **B)** The bar graph represents the quantitative analysis of basal respiration, ATP production, non-mitochondrial respiration, proton leak, maximal respiratory, and reserve respiratory capacity. Cell energy phenotype display shift toward glycolysis in *Alkbh8*^{def} MEFs. The data represents mean ± SEM, n = 5, *, $p \leq 0.1$, **, $p \leq 0.01$. **C)** Cell energy phenotype profile was obtained using XF report generator. All data are calculated and displayed as absolute OCR vs. absolute ECAR. Baseline OCR and ECAR (presented as open markers) are calculated from the last rate measurement before any injection and the stressed OCR and ECAR (presented as filled markers) represent the maximum rate measurement after FCCP injection.

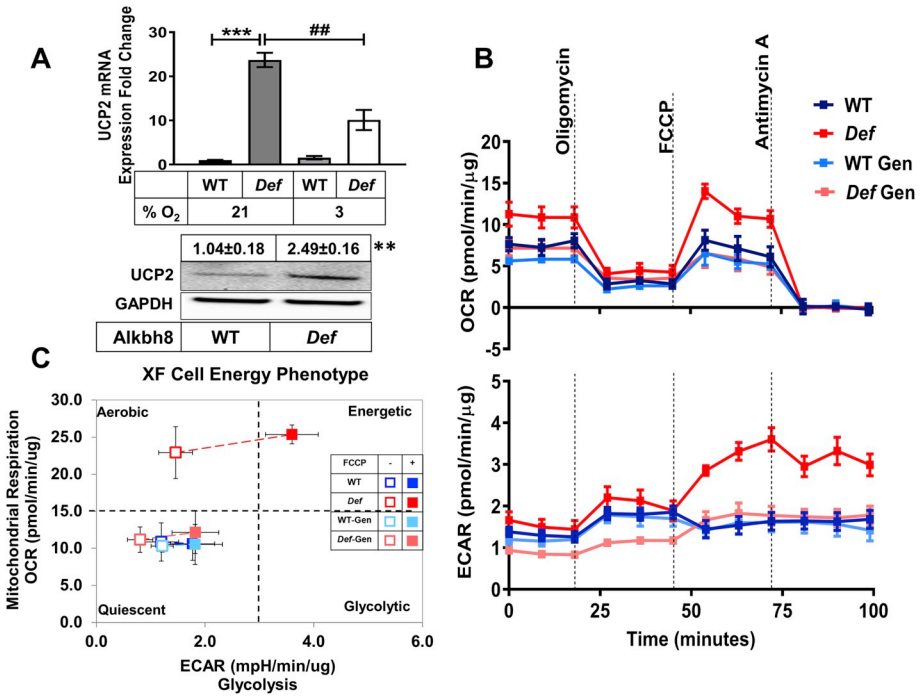

Fig. 6. *Alkbh8*^{def} drives UCP2 upregulation and augments metabolic flux. A) UCP2 expression in *Alkbh8*^{def} MEFs. All data was normalized to GAPDH controls and presented as mean ± SEM. ***, $p \leq 0.001$ when compared to WT, ##, $p = 0.003$ when compared to 21% O_2 *Alkbh8*^{def}. Inset, representative UCP2 immunoblot (n = 3) and densitometry obtained using ImageJ. **, $p \leq 0.01$ when compared to WT. **B)** Cell Mito Stress analysis as in Fig. 5 with n = 3 **C)** Cell energy phenotype as in Fig. 5 with n = 3.

not observed when cells were treated with genipin (Fig. 6C). These findings not only confirm that UCP2 is abundantly expressed in the *Alkbh8*^{def} cells but that its expression is of functional significance.

3.5. *Alkbh8*^{Def} *cells rely on glycolysis for survival and are resistant to arsenic containing mitochondrial toxins*

As the *Alkbh8*^{def} cells display a glycolytic adaptation in their cell energy phenotype, we evaluated their sensitivity to the glycolytic inhibitor 2-deoxyglucose (2DG). *Alkbh8*^{def} are significantly more sensitive to 2DG than their WT counterparts (Fig. 7A). In addition, while the *Alkbh8*^{def} MEFs display a proliferative defect to growth in ambient air, they are unusually resistant to a number of arsenicals which have been shown modulate mitochondrial ROS levels [40] (Supplementary Figure 5) and display self-sufficiency (high clonogenic activity) relative to WT MEFs that is blocked in response to 2DG treatment (Fig. 7B) which is reversed by Alkbh8 rescue (Supplementary Figure 6).

4. Discussion

Epitranscriptomic writer deficient cells adapt by engaging senescence, reprogramming stress response systems and altering mitochondrial function.

Our previous work demonstrated cellular senescence increases H_2O_2 production and engages the senescence associated secretory phenotype (SASP) [41–44]. Our objective here was to determine whether defects in an epitranscriptomic writer linked to Sec utilization leads to a similar redox-based activation of the senescent program. Here we report that selenoprotein loss resulting from *Alkbh8* deficiency limits H_2O_2 removal and engages the senescence program. Selenoprotein loss resulting from selenium restriction can also induce senescence which is reversed by selenium supplementation [24,45]. The *Alkbh8*^{def} mice may therefore be a good model to mimic a dietary loss of selenium. As *Alkbh8* deficiency increases DNA damage and enhances basal oxidant production [11], we first demonstrated that *Alkbh8*^{def} MEFs display a proliferative defect, which is reversed when cells are cultured in a low oxygen condition. The ability of low oxygen to delay senescence associated proliferative defects was first reported by Ames and confirmed by others [46,47] and similar to these reports the reversal of the growth

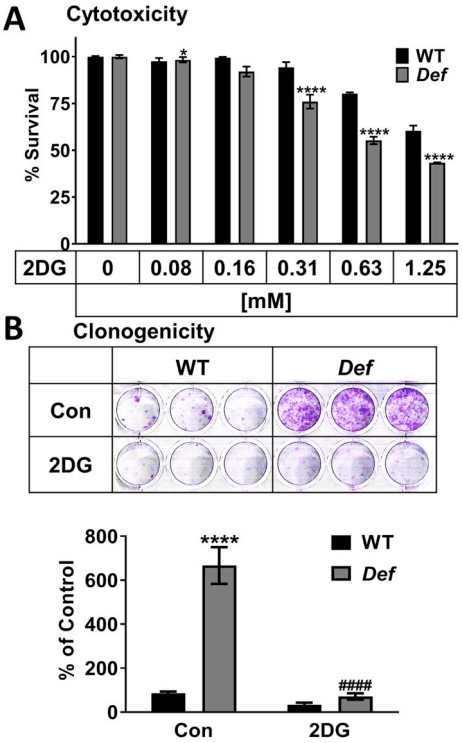

Fig. 7. *Alkbh8*^{def} increases sensitivity to glycolytic inhibition. A) Cytotoxicity assay using crystal violet stain was performed with 2DG treatment at various dosages for 24 h. **B)** Clonogenicity of WT and *Alkbh8*^{def} MEFs. The statistical comparison between untreated versus treated cells was presented as mean ± SEM, ****, $p \leq 0.0001$ and ####, $p \leq 0.0001$ compared to *Alkbh8*^{def} 2DG treated. (For interpretation of the references to colour in this figure legend, the reader is referred to the Web version of this article.)

impediment of the *Alkbh8*^{def} MEFs is likely attributed to reduction in metabolic H_2O_2.

While senescence engagement is only one mechanism by which cells adapt to oxidant burden, they often compensate by increasing

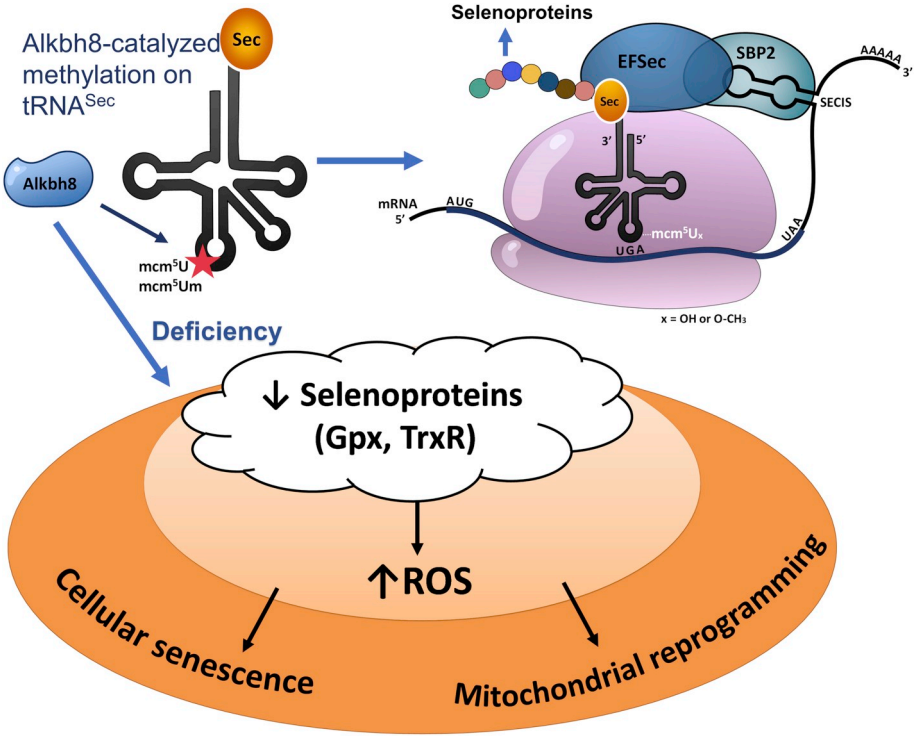

Fig. 8. Epitranscriptomic systems that regulate selenoprotein levels modulate senescence and mitochondrial function.

antioxidant enzyme levels or limiting mitochondrial electron leak [48]. The compensatory increase in many redox modifying genes is likely, in part, responsible for the enhanced stress resistance of *Alkbh8*^{def} cells. Interestingly many of these oxidant metabolizing systems are commonly upregulated during carcinogenesis, oncogenic transformation and metastatic disease [49].

Like senescent cells, *Alkbh8*^{def} MEFs display increased mitochondrial mass, ROS production, oxygen consumption and decrease ATP production [50]. A number of ALKBH family members have also been linked to defects in mitochondrial function. ALKBH1 is involved in biogenesis of 5-formyl-2′-O-methylcytidine (f5Cm) at position 34 and loss *Alkbh1* decreases mitochondrial translation and reduced respiratory complex activities [51]. ALKBH7 can trigger the collapse of mitochondrial membrane potential, energy depletion, and loss of mitochondrial function, which leads to oxidation induced programmed necrosis [52]. Thus, defects in the ALKBH family activity cause mitochondrial dysfunction with the potential to increase ROS production promote DNA damage and senescence growth arrest [53].

Mitochondria also cope with stress by controlling fusion/fission processes [54] and mitochondrial elongation is a common phenotype in response to energy stress involved in tumor cell survival [55]. The length of mitochondria and its dynamics are determined by the balance between fusion (MFN1, MFN2 and OPA1), and fission proteins (FIS1 and DRP1) [56,57]. The ratio of fusion and fission proteins is critical in disease-related processes such as apoptosis, mitophagy and cell survival [58]. Mitochondrial fusion has also been shown to play an important role in adapting to stress and increase in fusion events are correlated with senescence [34]. Loss of UCP2 is associated with an increase in fragmentation and decrease in the ratio of fusion/fission related proteins which is reversed by UCP2 overexpression [59], indicating that UCP2 may assist in driving the fusion processes. Our findings indicate that although no change was detected in MFN1 and MFN2 levels, *Alkbh8*^{def} MEFs display a significant decrease in the fission protein, DRP1, resulting in an increase of ratio of fusion and fission which likely promotes mitochondrial elongation. Whether this is a UCP2 mediated process remains to be determined.

Increased UCP2 has been reported to limit mitochondrial oxidant production and participate in many physiological processes including glucose and fatty acid utilization [60] and linked to type 2 diabetes and cancer [61–68]. Arsenic containing compounds are mitochondrial toxins that disrupt ATP production and are often lethal to normal cells [69,70]. Thus, increased UCP2 may promote survival of the *Alkbh8*^{def} MEFs in response to arsenic by limiting ROS production. Resistance to arsenic containing compounds but high sensitivity to 2DG indicates that glycolytic adaptation is also important to the survival of *Alkbh8*^{def} MEFs. While the proliferative capacity of *Alkbh8*^{def} MEFs is also impaired they display a significant survival advantage when grown at low seeding density compare to the WT MEFs. High clonogenic activity, stress resistance and a reliance on glycolysis for survival are key features of tumorigenic cell lines [71] and it is possible that conditions which limit ALKBH8 activity may potentiate tumorigenic activity.

4.1. Epitranscriptomic defects and adaptive phenotypes can be exploited to kill senescent cells

It is clear from our findings that cells adapt dramatically to the loss of ALKBH8 and defects in selenoprotein levels. In addition to mcm [5]U and mcm [5]Um modifications by ALKBH8, tRNA^{Sec} contains 2 modified bases at the T-arm, 1-methyladenosine (m^1A) at position 58 and pseudouridine (Ψ) at position 55, and one modified base at anti-codon arm, N [6]-isopentenyl-adenosine (i^6A) at position 37 [72]. m^1A modification is required for Ψ synthesis, which is essential for maintaining the tertiary structure of tRNA^{Sec} [73]. I^6A modification of tRNA$^{[Ser]Sec}$ catalyzed by tRNA isopentenyltransferase 1 (TRIT1) is required for decoding of UGA stop codon, as well as selenoproteins synthesis [74] and knock down of TRIT1 reduces selenoprotein expression [75]. Whether selenoprotein defects can engage cellular senescence and the relation between other epitranscriptomic modifications of tRNA^{Sec} and cellular senescence need to be further investigated.

Senescence has emerged as a key therapeutic target for many disease interventions as its abatement in distinct murine models limits age related decline in cognitive, cardiac and renal function, muscle atrophy,

cataracts and delays tumor burden [19,76]. Senescent abatement has been shown to delay atherosclerosis, pulmonary fibrosis, neurodegenerative disease, heart failure and tumor onset [15,77–81]. We demonstrate that the UCP2 inhibitor, genipin, negated increases in mitochondrial OCR in *Alkbh8*^{def} MEFs, as well as their glycolytic behavior. Our study is an early example of how an epitranscriptomic defect can be metabolically exploited to limit cell growth and may have potential applications in killing tumors with similar genetic profiles.

We have previously reported that the SASP is redox-regulated through a mechanism that involves redox-dependent transcriptional activation and impeding inhibitory signaling phosphatases [14]. Selenium deprivation has been established to engage senescent programming and our findings further support the importance of selenoproteins in this process likely through a similar redox based signaling process. Our study further indicates that additional, adaptive responses are engaged in response to selenoprotein deficiency. Senescence engagement coupled with stress resistance would create a microenvironment that is ripe for disease development and that targeting the epitranscriptome in combination with selenium supplementation may prove useful as a therapeutic strategy for disease intervention (See Fig. 8).

Funding

Research was funded by grants from the National Institutes of Health (Thomas Begley - R01ES026856 and R01ES024615) and SUNY Polytechic Institute COR Seed Grant (J. Andres Melendez - 1147718).

Appendix A. Supplementary data

Supplementary data to this article can be found online at https://doi.org/10.1016/j.redox.2019.101375.

References

[1] Morena, F., Argentati, C., Bazzucchi, M., Emiliani, C. & Martino, S. Above the Epitranscriptome: RNA Modifications and Stem Cell Identity. doi:10.3390/genes9070329.
[2] M. Esteller, P.P. Pandolfi, B. Israel, The epitranscriptome of non-coding RNAs in cancer HHS public access, Cancer Discov. 7 (2017) 359–368.
[3] A.G. Torres, E. Batlle, L. Ribas de Pouplana, Role of tRNA modifications in human diseases, Trends Mol. Med. 20 (2014) 306–314.
[4] S. Huber, A. Leonardi, P. Dedon, T. Begley, The versatile roles of the tRNA epitranscriptome during cellular responses to toxic exposures and environmental stress, Toxics 7 (2019) 17.
[5] L. Trixl, A. Lusser, The dynamic RNA modification 5-methylcytosine and its emerging role as an epitranscriptomic mark, Wiley Interdiscip. Rev. RNA 10 (2019) 1–17.
[6] M.T. Bohnsack, K.E. Sloan, The mitochondrial epitranscriptome: the roles of RNA modifications in mitochondrial translation and human disease, Cell. Mol. Life Sci. 75 (2018) 241–260.
[7] D. Fu, et al., Human AlkB homolog ABH8 Is a tRNA methyltransferase required for wobble uridine modification and DNA damage survival, Mol. Cell. Biol. 30 (2010) 2449–2459.
[8] L. Songe-Moller, et al., Mammalian ALKBH8 possesses tRNA methyltransferase activity required for the biogenesis of multiple wobble uridine modifications implicated in translational decoding, Mol. Cell. Biol. 30 (2010) 1814–1827.
[9] H. Hori, Methylated nucleosides in tRNA and tRNA methyltransferases, Front. Genet. 5 (2014) 1–26.
[10] A. Böck, et al., Selenocysteine: the 21st amino acid, Mol. Microbiol. 5 (1991) 515–520.
[11] L. Endres, et al., Alkbh8 regulates selenocysteine-protein expression to protect against reactive oxygen species damage, PLoS One 10 (2015) e0131335.
[12] J. Campisi, Senescent cells, tumor suppression, and organismal aging: good citizens, bad neighbors, Cell 120 (2005) 513–522.
[13] B.G. Childs, et al., Senescent cells: an emerging target for diseases of ageing, Nat. Rev. Drug Discov. 16 (2017) 718–735.
[14] D.A. McCarthy, R.R. Clark, T.R. Bartling, M. Trebak, J.A. Melendez, Redox control of the senescence regulator interleukin-1α and the secretory phenotype, J. Biol. Chem. 288 (2013) 32149–32159.
[15] T. Kadota, et al., Emerging role of extracellular vesicles as a senescence-associated secretory phenotype: insights into the pathophysiology of lung diseases, Mol. Asp. Med. 60 (2018) 92–103.
[16] J.-P. Coppé, et al., Senescence-associated secretory phenotypes reveal cell-non-autonomous functions of oncogenic RAS and the p53 tumor suppressor, PLoS Biol. 6 (2008) 2853–2868.
[17] J.-P. Coppé, P.-Y. Desprez, A. Krtolica, J. Campisi, The senescence-associated secretory phenotype: the dark side of tumor suppression, Annu. Rev. Pathol. 5 (2010) 99–118.
[18] T. Tchkonia, Y. Zhu, J. van Deursen, J. Campisi, J.L. Kirkland, Cellular senescence and the senescent secretory phenotype: therapeutic opportunities, J. Clin. Investig. 123 (2013) 966–972.
[19] P.A. Pérez-Mancera, A.R.J. Young, M. Narita, Inside and out: the activities of senescence in cancer, Nat. Rev. Cancer 14 (2014) 547–558.
[20] R.M. Naylor, D.J. Baker, J.M. van Deursen, Senescent cells: a novel therapeutic target for aging and age-related diseases, Clin. Pharmacol. Ther. 93 (2013) 105–116.
[21] J. Campisi, Aging, cellular senescence, and cancer, Annu. Rev. Physiol. 75 (2013) 685–705.
[22] E.H. Bent, L.A. Gilbert, M.T. Hemann, A senescence secretory switch mediated by PI3K/AKT/mTOR activation controls chemoprotective endothelial secretory responses, Genes Dev. 30 (2016) 1811–1821.
[23] P.J. Hornsby, S.E. Harris, Oxidative damage to DNA and replicative lifespan in cultured adrenocortical cells, Exp. Cell Res. 168 (1987) 203–217.
[24] Y. Legrain, Z. Touat-Hamici, L. Chavatte, Interplay between selenium levels, selenoprotein expression, and replicative senescence in WI-38 human fibroblasts, J. Biol. Chem. 289 (2014) 6299–6310.
[25] G. Hammad, et al., Interplay between selenium levels and replicative senescence in WI-38 human fibroblasts: a proteomic approach, Antioxidants (Basel, Switzerland) 7 (2018).
[26] E. Mocchegiani, et al., Zinc, metallothioneins and longevity: interrelationships with niacin and selenium, Curr. Pharmaceut. Des. 14 (2008) 2719–2732.
[27] N.T. Akbaraly, et al., Selenium and mortality in the Elderly : results from the EVA study, Gen. Clin. Chem. 2123 (2005) 2117–2123.
[28] R. Alis, et al., Trace elements levels in centenarian 'dodgers', J. Trace Elem. Med. Biol. 35 (2016) 103–106.
[29] L. Zhang, H. Zeng, W.-H. Cheng, Beneficial and paradoxical roles of selenium at nutritional levels of intake in healthspan and longevity, Free Radic. Biol. Med. 127 (2018) 3–13.
[30] R.K. Dagda, M. Rice, R.A. Merrill, K.H. Flippo, S. Strack, Techniques to investigate mitochondrial function in neurons, Neuromethods 123 (2017) 1–27.
[31] A.J. Valente, L.A. Maddalena, E.L. Robb, F. Moradi, J.A. Stuart, A simple ImageJ macro tool for analyzing mitochondrial network morphology in mammalian cell culture, Acta Histochem. 119 (2017) 315–326.
[32] G.P. Dimri, et al., A biomarker that identifies senescent human-cells in culture and in aging skin in-vivo, Proc. Natl. Acad. Sci. U.S.A. 92 (1995) 9363–9367.
[33] D.J. Baker, et al., Naturally occurring p16Ink4a-positive cells shorten healthy lifespan, Nature 530 (2016) 184–189.
[34] D.V. Ziegler, C.D. Wiley, M.C. Velarde, Mitochondrial effectors of cellular senescence: beyond the free radical theory of aging, Aging Cell 14 (2015) 1–7.
[35] P. Dalle Pezze, et al., Dynamic modelling of pathways to cellular senescence reveals strategies for targeted interventions, PLoS Comput. Biol. 10 (2014).
[36] L.C. Gomes, G. Di Benedetto, L. Scorrano, During autophagy mitochondria elongate, are spared from degradation and sustain cell viability, Nat. Cell Biol. 13 (2011) 589–598.
[37] J.F. Passos, et al., Feedback between p21 and reactive oxygen production is necessary for cell senescence, Mol. Syst. Biol. 6 (2010) 347.
[38] M.D. Brand, T.C. Esteves, Physiological functions of the mitochondrial uncoupling proteins UCP2 and UCP3, Cell Metabol. 2 (2005) 85–93.
[39] I.K. Hals, et al., Marked over expression of uncoupling protein-2 in beta cells exerts minor effects on mitochondrial metabolism, Biochem. Biophys. Res. Commun. 423 (2012) 259–264.
[40] C. Blajszczak, M.G. Bonini, Mitochondria targeting by environmental stressors: implications for redox cellular signaling, Toxicology 391 (2017) 84–89.
[41] A.C. Ranganathan, et al., Manganese superoxide dismutase signals matrix metalloproteinase expression via H2O2-dependent ERK1/2 activation, J. Biol. Chem. 276 (2001) 14264–14270.
[42] K.K. Nelson, et al., Elevated sod2 activity augments matrix metalloproteinase expression: evidence for the involvement of endogenous hydrogen peroxide in regulating metastasis, Clin. Cancer Res. 9 (2003) 424–432.
[43] K.K. Nelson, et al., Redox-dependent matrix metalloproteinase-1 expression is regulated by JNK through Ets and AP-1 promoter motifs, J. Biol. Chem. 281 (2006) 14100–14110.
[44] J. Dasgupta, et al., Reactive oxygen species control senescence-associated matrix metalloproteinase-1 through c-Jun-N-terminal kinase, J. Cell. Physiol. 225 (2010) 52–62.
[45] I. Sadowska-Bartosz, G. Bartosz, Effect of Antioxidants Supplementation on Aging and Longevity, (2014), https://doi.org/10.1155/2014/404680.
[46] J. Dasgupta, et al., Reactive oxygen species control senescence-associated matrix metalloproteinase-1 through c-Jun-N-terminal kinase, J. Cell. Physiol. 225 (2010) 52–62.
[47] M.K. Shigenaga, T.M. Hagen, B.N. Ames, Oxidative damage and mitochondrial decay in aging, Proc. Natl. Acad. Sci. U.S.A. 91 (1994) 10771–10778.
[48] L.A. Sena, N.S. Chandel, Physiological Roles of Mitochondrial Reactive Oxygen Species, (2012), https://doi.org/10.1016/j.molcel.2012.09.025.
[49] G. Pani, T. Galeotti, P. Chiarugi, Metastasis: cancer cell's escape from oxidative stress, Cancer Metastasis Rev. 29 (2010) 351–378.
[50] V.I. Korolchuk, S. Miwa, B. Carroll, T. von Zglinicki, Mitochondria in cell senescence: is mitophagy the weakest link? EBioMedicine (2017), https://doi.org/10.1016/j.ebiom.2017.03.020.
[51] T.A. Müller, S.L. Struble, K. Meek, R.P. Hausinger, Characterization of human AlkB homolog 1 produced in mammalian cells and demonstration of mitochondrial

dysfunction in ALKBH1-deficient cells, Biochem. Biophys. Res. Commun. 495 (2018) 98–103.
[52] D. Fu, J.J. Jordan, L.D. Samson, Human ALKBH7 is required for alkylation and oxidation-induced programmed necrosis, Genes Dev. 27 (2013) 1089–1100.
[53] J. Kaplon, et al., A key role for mitochondrial gatekeeper pyruvate dehydrogenase in oncogene-induced senescence, Nature 498 (2013) 109–112.
[54] J. Suárez-Rivero, et al., Mitochondrial dynamics in mitochondrial diseases, Diseases 5 (2016) 1.
[55] J. Li, et al., Mitochondrial elongation-mediated glucose metabolism reprogramming is essential for tumour cell survival during energy stress, Oncogene 36 (2017) 4901–4912.
[56] B. Westermann, Mitochondrial fusion and fission in cell life and death, Nat. Rev. Mol. Cell Biol. 11 (2010) 872–884.
[57] L. Simula, F. Nazio, S. Campello, The mitochondrial dynamics in cancer and immune-surveillance, Semin. Cancer Biol. 47 (2017) 29–42.
[58] A.M. van der Bliek, Q. Shen, S. Kawajiri, Mechanisms of mitochondrial fission and fusion, Cold Spring Harb. Perspect. Biol. 5 (2013) a011072–a011072.
[59] Y. Shimasaki, et al., Uncoupling protein 2 impacts endothelial phenotype via p53-mediated control of mitochondrial dynamics, Circ. Res. 113 (2013) 891–901.
[60] C. Pecqueur, C. Alves-Guerra, D. Ricquier, F. Bouillaud, UCP2, a metabolic sensor coupling glucose oxidation to mitochondrial metabolism? IUBMB Life 61 (2009) 762–767.
[61] J.S. Moon, et al., UCP2-induced fatty acid synthase promotes NLRP3 inflammasome activation during sepsis, J. Clin. Investig. 125 (2015) 665–680.
[62] V. Ayyasamy, et al., Cellular model of warburg effect identifies tumor promoting function of UCP2 in breast cancer and its suppression by genipin, PLoS One 6 (2011) e24792.
[63] J. Su, et al., Cytoprotective effect of the UCP2-SIRT3 signaling pathway by decreasing mitochondrial oxidative stress on cerebral ischemia–reperfusion injury, Int. J. Mol. Sci. 18 (2017).
[64] N. Tsuboyama-Kasaoka, K. Sano, C. Shozawa, T. Osaka, O. Ezaki, Studies of UCP2 transgenic and knockout mice reveal that liver UCP2 is not essential for the anti-obesity effects of fish oil, Am. J. Physiol. Endocrinol. Metab. 294 (2008) E600–E606.
[65] N. Li, M. Karaca, P. Maechler, Upregulation of UCP2 in beta-cells confers partial protection against both oxidative stress and glucotoxicity, Redox Biol. 13 (2017) 541–549.
[66] M.A. Pitt, Overexpression of uncoupling protein-2 in cancer: metabolic and heat changes, inhibition and effects on drug resistance, Inflammopharmacology 23 (2015) 365–369.
[67] C.Y. Zhang, et al., Uncoupling protein-2 negatively regulates insulin secretion and is a major link between obesity, beta cell dysfunction, and type 2 diabetes, Cell 105 (2001) 745–755.
[68] H.Y. Lim, et al., Metabolic signatures of renal cell carcinoma, Biochem. Biophys. Res. Commun. 460 (2015) 938–943.
[69] C.H. Tseng, The potential biological mechanisms of arsenic-induced diabetes mellitus, Toxicol. Appl. Pharmacol. 197 (2004) 67–83.
[70] A.P. Singh, R.K. Goel, T. Kaur, Mechanisms pertaining to arsenic toxicity, Toxicol. Int. 18 (2011) 87–93.
[71] N.A.P. Franken, H.M. Rodermond, J. Stap, J. Haveman, C. van Bree, Clonogenic assay of cells in vitro, Nat. Protoc. 1 (2006) 2315–2319.
[72] J.N. Gonzalez-Flores, S.P. Shetty, A. Dubey, P.R. Copeland, The molecular biology of selenocysteine, Biomol. Concepts 4 (2013) 349–365.
[73] L.K. Kim, et al., Methylation of the ribosyl moiety at position 34 of selenocysteine tRNA[Ser]Sec is governed by both primary and tertiary structure, RNA (2000) 1306–1315.
[74] G.J. Warner, et al., Inhibition of selenoprotein synthesis by selenocysteine tRNA([Ser]Sec) lacking isopentenyladenosine, J. Biol. Chem. 275 (2000) 28110–28119.
[75] N. Fradejas, et al., Mammalian Trit1 is a tRNA [Ser]Sec -isopentenyl transferase required for full selenoprotein expression, Biochem. J. 450 (2013) 427–432.
[76] A. Chandrasekaran, M.D.P.S. Idelchik, J.A. Melendez, Redox control of senescence and age-related disease, Redox Biol. 11 (2017) 91–102.
[77] K. Shinmura, Cardiac senescence, heart failure, and frailty: a triangle in elderly people, Keio J. Med. 65 (2016) 25–32.
[78] M. Chilosi, A. Carloni, A. Rossi, V. Poletti, Premature lung aging and cellular senescence in the pathogenesis of idiopathic pulmonary fibrosis and COPD/emphysema, Transl. Res. 162 (2013) 156–173.
[79] A.R. Mendelsohn, J.W. Larrick, Cellular senescence as the key intermediate in tau-mediated neurodegeneration, Rejuvenation Res. 21 (2018) 572–579.
[80] I. Shimizu, et al., p53-Induced adipose tissue inflammation is critically involved in the development of insulin resistance in heart failure, Cell Metabol. 15 (2012) 51–64.
[81] X. Zhou, F. Perez, K. Han, D.A. Jurivich, Clonal senescence alters endothelial ICAM-1 function, Mech. Ageing Dev. 127 (2006) 779–785.